# A vertex-based scheme on polyhedral meshes for advection-reaction equations with sub-mesh stabilization

Jérôme Bonelle [*,1], Erik Burman [†,2], Pierre Cantin [‡,1,3], and Alexandre Ern [§,3]

[1]EDF R&D, 6 quai Watier, 78401 Chatou BP 49, France
[2]Dept. of Mathematics, University College London, Gower Street, London, UK
[3]Université Paris-Est, CERMICS (ENPC), 77455 Marne la Vallée Cedex 2, France

## Abstract

We devise and analyze vertex-based schemes on polyhedral meshes to approximate advection-reaction equations. Error estimates of order $O(h^{3/2})$ are established in the discrete inf-sup stability norm which includes the mesh-dependent weighted advective derivative. The two key ingredients are a local polyhedral reconstruction map leaving affine polynomials invariant, and a local design of stabilization whereby gradient jumps are only penalized across some subfaces in the interior of each mesh cell. Numerical results are presented on three-dimensional polyhedral meshes.

**AMS Subject Classification.** 65N12, 65N30, 65N08

## 1 Introduction

Considering a polyhedral domain $\Omega$ in $\mathbb{R}^3$, we want to approximate the scalar-valued function $p : \Omega \to \mathbb{R}$ solving the following first-order problem:

$$\boldsymbol{\beta}\cdot\nabla p + \mu p = s \quad \text{a.e. in} \ \ \Omega, \tag{1.1a}$$

$$p = p_D \ \text{a.e. on} \ \partial\Omega^-, \tag{1.1b}$$

where $\boldsymbol{\beta} \in \mathbf{Lip}(\Omega)$ is a given vector-field and $\mu \in L^\infty(\Omega)$ a reaction coefficient. The forcing term is such that $s \in L^2(\Omega)$, and we assume that $p_D \in H^t(\partial\Omega)$ with $t > 1$; more generally, it is possible to consider a piecewise smooth boundary datum $p_D$ on a given partition of the boundary provided the boundary mesh is fitted to this partition. Dirichlet boundary conditions are enforced on the inflow part of the boundary $\partial\Omega^-$, where $\partial\Omega^\pm = \{\boldsymbol{x} \in \partial\Omega \,|\, \pm\boldsymbol{\beta}(\boldsymbol{x})\cdot\boldsymbol{n} > 0\}$ and $\boldsymbol{n}$ is the unit outward normal. We assume that there exists a reference time $\tau > 0$ such that $\mu - \frac{1}{2}\nabla\cdot\boldsymbol{\beta} \geq \tau^{-1}$ holds a.e. on $\Omega$. In the above setting, the problem (1.1) is well posed; see, e.g., [14].

Our first goal is to devise and analyze a discretization scheme for (1.1) that supports general meshes including polyhedral cells and nonmatching interfaces. Such meshes are

---

[*]Email : jerome.bonelle@edf.fr
[†]Email : e.burman@ucl.ac.uk
[‡]Email : pircantin@gmail.com
[§]Email : alexandre.ern@enpc.fr

indeed important in many applications involving multi-physics and multi-domain problems and also in computer graphics and topology optimization. General meshes also allow for more flexibility when meshing complex geometries by using cells of different geometric shapes, and provide a natural setting to handle nonmatching interfaces. Our second goal is to consider vertex-based schemes, i.e., schemes with degrees of freedom (DoFs) attached to the mesh vertices, and to achieve $O(h^{3/2})$ convergence rates for smooth solutions where $h$ denotes the mesh-size. Vertex-based schemes are attractive since they provide a natural way to discretize 0-differential forms (i.e., potentials) in the context of differential geometry. Moreover, compared to discontinuous Galerkin methods [23, 22, 14, 12] which are cell-based schemes, using one DoF per vertex is, in general, more effective than using piecewise affine functions, i.e., four DoFs per cell, to achieve $O(h^{3/2})$ accuracy.

To the best of the authors' knowledge, there are no vertex-based schemes of order $O(h^{3/2})$ on polyhedral meshes available in the literature for the advection-reaction problem (1.1). Instead, many examples of stabilized $\mathbb{P}_1$ Lagrange finite elements can be found on (matching) simplicial meshes; among various choices for stabilization, we mention Streamline Diffusion [21], Subgrid Viscosity [19, 20], Continuous Interior Penalty (CIP) [7, 9, 8], and Local Projection Stabilization [3, 6, 24, 25]. Thus, the present work can be viewed as a polyhedral extension of stabilized finite elements. We also mention that the present scheme for the advection-reaction problem (1.1) can be combined with the recent Compatible Discrete Operator (CDO) schemes for diffusion problems from [5], so as to discretize advection-diffusion problems in a Péclet-robust manner on polyhedral meshes. A recent Péclet-robust CDO scheme for advection-diffusion on polyhedral meshes has been analyzed in [11]; therein, however, the convergence rate is only of order $O(h^{1/2})$ in the advection-dominated regime (and $O(h)$ in the diffusion-dominated regime). Therefore, the present work can also be viewed as a higher-order extension of [11]. Furthermore, the present scheme can also be combined with the recent Vertex-Approximate Gradient schemes for diffusion [16, 17, 18] and, therefore, provide a higher-order alternative to the more usual finite-volume treatment of advection based on upwinding.

The main idea to devise our scheme consists of introducing, in addition to the vertex-based DoFs, one DoF per mesh cell. The additional cell DoFs can be eliminated locally using a Schur complement technique (i.e., static condensation). Since cell DoFs are uncoupled from each other (and are only coupled to vertex-based DoFs), this elimination entails modest marginal costs since no matrix inversion is required. The main benefit is that the size of the linear system to be solved is just the number of mesh vertices. Our first important ingredient is the introduction of a polyhedral reconstruction map defining $\mathbb{P}_1$ broken polynomials on each mesh cell from the local vertex and cell DoFs. Our second important ingredient is the stabilization. A crucial point is to devise the stabilization locally so that it does not hamper the possibility of eliminating locally the cell DoFs. In the present work, we achieve this by using CIP stabilization, but we penalize the gradient jump only across some interior subfaces of each mesh cell. As shown recently in [10] in a different context related to composite elements, the CIP technique provides enough stabilization. Our main result is Theorem 3.7. Its proof hinges essentially on two intermediate results: discrete inf-sup stability and a bound on the consistency error. The former hinges on using the advective derivative as test function, but only for the cell DoFs, similarly in spirit to [10]. The latter hinges on the design of the polyhedral reconstruction map that leaves affine polynomials locally invariant.

The material is organized as follows. In section 2, we introduce the discrete setting. In section 3, we present the main results in the analysis; the proofs, along with some technical

results, are postponed to Section 5. In section 4, we detail some implementation aspects and we present numerical results on three-dimensional polyhedral meshes.

## 2 Discrete setting

In this section, we introduce some basic notation concerning polyhedral meshes and we define the local reconstruction maps as well as the discrete scheme.

### 2.1 Meshes

We consider a mesh M of the domain $\Omega \subset \mathbb{R}^3$ composed of (possibly) polyhedral cells $c \in C$, planar faces $f \in F$, straight edges $e \in E$, and vertices $v \in V$. By convention, all the cells, faces, and edges of the mesh are closed sets in $\mathbb{R}^3$. Since boundary conditions are weakly enforced, we also consider the subset $F^\partial = \{f \in F \,|\, f \subset \partial\Omega\}$ composed of the boundary faces. We denote by # the cardinal number of a set, so that #V is equal to the number of vertices of M, #E to the number of edges, and so on.

The quadruple $\{V, E, F, C\}$ is a cellular complex in the sense that the boundary of a cell in C is composed of faces in F, that of a face in F is composed of edges in E, and that of an edge in E of (two) vertices in V. For two types of mesh entities $A, X \in \{V, E, F, C\}$, letting $a \in A$, we denote by $X_a$ the set defined as $\{x \in X \,|\, a \subset \partial x\}$ if the dimension of $a$ is smaller than that of elements of X and as $X_a = \{x \in X \,|\, x \subset \partial a\}$ otherwise. Important examples are the sets $F_c = \{f \in F \,|\, f \subset \partial c\}$, $E_f = \{e \in E \,|\, e \subset \partial f\}$, $C_f = \{c \in C \,|\, f \subset \partial c\}$.

We denote by $\boldsymbol{x}_v$, $\boldsymbol{x}_e$, $\boldsymbol{x}_f$, and $\boldsymbol{x}_c$ the barycenters of $v \in V$, $e \in E$, $f \in F$, and $c \in C$ respectively. We assume that $f$ and $c$ are star-shaped with respect to $\boldsymbol{x}_f$ and $\boldsymbol{x}_c$, respectively. Each polyhedral cell $c \in C$ is subdivided into elementary simplices $\mathfrak{p}_{ef,c} := [\boldsymbol{x}_{v_1}, \boldsymbol{x}_{v_2}, \boldsymbol{x}_f, \boldsymbol{x}_c]$ (the brackets denote the convex cell) for all $f \in F_c$ and all $e \in E_f$ with $e = [\boldsymbol{x}_{v_1}, \boldsymbol{x}_{v_2}]$; see the left panel of Figure 1. This partition of the cell, which plays a central role in this work, is denoted

$$\mathfrak{P}_c = \cup_{f \in F_c} \cup_{e \in E_f} \mathfrak{p}_{ef,c}.$$

Note that $\#\mathfrak{P}_c = 2\#E_c$ since each mesh edge is shared by two mesh faces. Another useful partition of the cell $c$ is composed of the polyhedra

$$\mathfrak{p}_{v,c} := \bigcup_{f \in F_c \cap F_v} \bigcup_{e \in E_f \cap E_v} [\boldsymbol{x}_v, \boldsymbol{x}_e, \boldsymbol{x}_f, \boldsymbol{x}_c]$$

for all $v \in V_c$; see the right panel of Figure 1. Notice that under the above star-shaped assumption, $c = \cup_{f \in F_c} \cup_{e \in E_f} \mathfrak{p}_{ef,c}$ and $c = \bigcup_{v \in V_c} \mathfrak{p}_{v,c}$ as sets of points in $\mathbb{R}^3$.

In what follows, we consider families of polyhedral meshes satisfying the following regularity criterion.

(**M**) $\#E_c$ is uniformly bounded and the simplices composing $\mathfrak{P}_c$ are shape-regular in the usual sense.

### 2.2 Degrees of freedom

We consider degrees of freedom (DoFs) attached to mesh vertices and mesh cells. Let $\mathcal{V} \equiv \mathbb{R}^{\#V}$ and $\mathcal{C} \equiv \mathbb{R}^{\#C}$ be the finite-dimensional spaces collecting the degrees of freedom attached to vertices and cells, respectively. We define the product space $\mathcal{P} = \mathcal{V} \times \mathcal{C}$, and
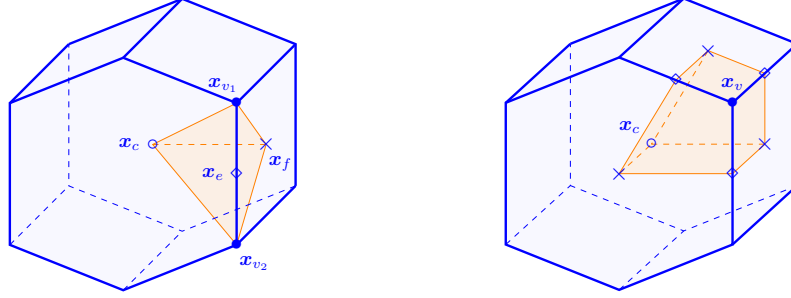
Figure 1: Left, simplex $\mathfrak{p}_{ef,c}$. Right, polyhedron $\mathfrak{p}_{v,c}$.

use the notation $\mathsf{p} = (\mathsf{p}_{\mathcal{V}}, \mathsf{p}_{\mathcal{C}}) \in \mathcal{P}$. We denote by $\mathsf{p}_v$ and $\mathsf{p}_c$ the entries of the vector $\mathsf{p}$ attached to the vertex $v \in V$ and to the cell $c \in C$, respectively.

It is convenient to localize discrete objects to a cell of the mesh. Let $c \in C$ and recall the local subset $V_c = \{v \in V \,|\, v \subset c\}$ containing the vertices of $c$. The vector space $\mathcal{P}_c \equiv \mathbb{R}^{\#V_c+1}$ is then composed of vectors of the form $\mathsf{p} = ((\mathsf{p}_v)_{v \in V_c}, \mathsf{p}_c)$.

*Remark* 2.1 (Simplicial submesh). Putting together all the partitions of the polyhedral mesh cells leads to a global simplicial mesh of the domain. Using a standard simplicial finite element method on that mesh would, however, be more expensive than using the present method since it entails attaching discrete unknowns to mesh vertices, faces, and cells.

## 2.3 Local reconstruction map

The central ingredient in our work is a reconstruction map $\mathsf{L}_{\mathcal{P}_c}$ that allows us to build locally in each mesh cell $c \in C$ a function from local DoFs $\mathsf{p} \in \mathcal{P}_c$. The reconstructed function $\mathsf{L}_{\mathcal{P}_c}(\mathsf{p})$ is continuous in $c$ and is piece-wise affine on the partition $\mathfrak{P}_c$ of $c$. To define the function $\mathsf{L}_{\mathcal{P}_c}(\mathsf{p})$, we consider the usual Courant (or hat) basis functions associated with the simplicial partition $\mathfrak{P}_c$ of $c$; we denote these functions as

$$((\theta_v)_{v \in V_c}, (\theta_f)_{f \in F_c}, \theta_c).$$

Observe that $\theta_c$ is a bubble function in the sense that it vanishes on the boundary of $c$. We then set, for all $\mathsf{p} \in \mathcal{P}_c$,

$$\mathsf{L}_{\mathcal{P}_c}(\mathsf{p})(\boldsymbol{x}) := \sum_{v \in V_c} \mathsf{p}_v \ell_{v,c}(\boldsymbol{x}) + \mathsf{p}_c \ell_c(\boldsymbol{x}), \qquad \forall \boldsymbol{x} \in c, \tag{2.1}$$

with the local reconstruction functions $((\ell_{v,c})_{v \in V_c}, \ell_c)$ such that

$$\ell_{v,c} := \theta_v + \sum_{f \in F_v} \frac{|f \cap \mathfrak{p}_{v,c}|}{|f|} \theta_f, \; \forall v \in V_c, \qquad \ell_c := \theta_c. \tag{2.2}$$

## 2.4 Discrete scheme

The discrete problem consists in finding $\mathsf{p} \in \mathcal{P}$ such that, for all $\mathsf{q} \in \mathcal{P}$,

$$\mathsf{A}(\mathsf{p}, \mathsf{q}) + \mathsf{A}^{\partial}(\mathsf{p}, \mathsf{q}) = \Xi(s, p_D; \mathsf{q}), \tag{2.3}$$

where the bilinear form $\mathsf{A} : \mathcal{P} \times \mathcal{P} \to \mathbb{R}$ results from the Galerkin approximation plus a local stabilization and the bilinear form $\mathsf{A}^\partial : \mathcal{P} \times \mathcal{P} \to \mathbb{R}$ weakly enforces the boundary condition, while the linear form $\Xi(s, p_D; \cdot) : \mathcal{P} \to \mathbb{R}$ accounts for the problem data.

The bilinear form $\mathsf{A}$ is assembled cell-wise as

$$\mathsf{A}(\mathsf{p}, \mathsf{q}) := \sum_{c \in \mathrm{C}} \mathsf{A}_c(\mathsf{p}, \mathsf{q}), \tag{2.4}$$

with a slight abuse of notation since we still denote by $\mathsf{p}$ the restriction of an element of $\mathcal{P}$ to $\mathcal{P}_c$. The local bilinear form $\mathsf{A}_c : \mathcal{P}_c \times \mathcal{P}_c \to \mathbb{R}$ is defined by means of the local reconstruction map $\mathsf{L}_{\mathcal{P}_c}$ as follows:

$$\mathsf{A}_c(\mathsf{p}, \mathsf{q}) := \mathsf{a}_c(\mathsf{p}, \mathsf{q}) + \gamma \, \mathsf{s}_c(\mathsf{p}, \mathsf{q}), \tag{2.5a}$$

$$\mathsf{a}_c(\mathsf{p}, \mathsf{q}) := \int_c \boldsymbol{\beta} \cdot \nabla \mathsf{L}_{\mathcal{P}_c}(\mathsf{p}) \, \mathsf{L}_{\mathcal{P}_c}(\mathsf{q}) + \int_c \mu \, \mathsf{L}_{\mathcal{P}_c}(\mathsf{p}) \, \mathsf{L}_{\mathcal{P}_c}(\mathsf{q}), \tag{2.5b}$$

$$\mathsf{s}_c(\mathsf{p}, \mathsf{q}) := h_c^2 |\boldsymbol{\beta}_c|^{-1} \sum_{\mathfrak{f} \in \mathfrak{F}_c} \int_{\mathfrak{f}} (\boldsymbol{\beta}_c \cdot [\![ \nabla \mathsf{L}_{\mathcal{P}_c}(\mathsf{p}) ]\!]) \, (\boldsymbol{\beta}_c \cdot [\![ \nabla \mathsf{L}_{\mathcal{P}_c}(\mathsf{q}) ]\!]), \tag{2.5c}$$

where $\gamma > 0$ is a stabilization parameter, $h_c$ denotes the diameter of the mesh cell $c$, $\boldsymbol{\beta}_c := \boldsymbol{\beta}(\boldsymbol{x}_c)$, and $|\boldsymbol{\beta}_c| := \|\boldsymbol{\beta}_c\|_{\ell^2(\mathbb{R}^3)}$. Moreover, $\mathfrak{F}_c$ is the set composed of the internal subfaces in $c$ resulting from the simplicial partition $\mathfrak{P}_c$ of $c$, that is, $\mathfrak{F}_c = \{\mathfrak{f} \subset \partial \mathfrak{p} \mid \mathfrak{p} \in \mathfrak{P}_c, \, \mathfrak{f} \not\subset \partial c\}$, see Figure 2, and $[\![ \mathsf{q} ]\!]$ denotes the jump of $\mathsf{q}$ across each face $\mathfrak{f} \in \mathfrak{F}_c$ defined by $\mathsf{q}_{|\mathfrak{p}_1} - \mathsf{q}_{|\mathfrak{p}_2}$ with $\mathfrak{f} = \partial \mathfrak{p}_1 \cap \partial \mathfrak{p}_2$.
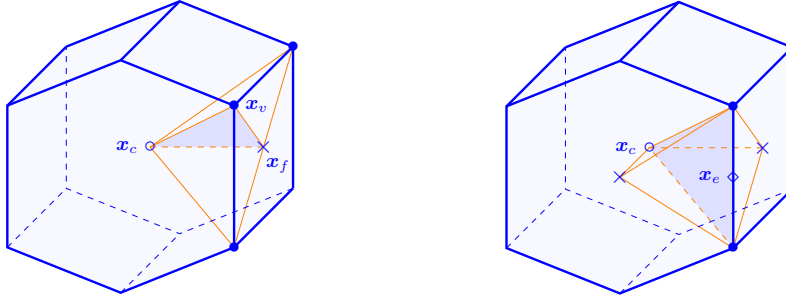


Figure 2: Two internal subfaces contained in the set $\mathfrak{F}_c$ and attached to the sub-mesh $\mathfrak{P}_c$.

The bilinear form weakly enforcing the boundary condition is assembled face-wise as

$$\mathsf{A}^\partial(\mathsf{p}, \mathsf{q}) := \sum_{f \in \mathrm{F}^\partial} \mathsf{A}_f^\partial(\mathsf{p}, \mathsf{q}) \tag{2.6}$$

where, letting $c_f$ be the unique cell of which $f$ is a face, we have

$$\mathsf{A}_f^\partial(\mathsf{p}, \mathsf{q}) := \int_f (\boldsymbol{\beta} \cdot \boldsymbol{n})^- \, \mathsf{L}_{\mathcal{P}_{c_f}}(\mathsf{p}) \, \mathsf{L}_{\mathcal{P}_{c_f}}(\mathsf{q}), \tag{2.7}$$

with $(\boldsymbol{\beta} \cdot \boldsymbol{n})^- := \frac{1}{2}(|\boldsymbol{\beta} \cdot \boldsymbol{n}| - \boldsymbol{\beta} \cdot \boldsymbol{n})$. Finally, the linear form $\Xi$ is such that

$$\Xi(s, p_D; \mathsf{q}) := \sum_{c \in \mathrm{C}} \int_c s \, \mathsf{L}_{\mathcal{P}_c}(\mathsf{q}) + \sum_{f \in \mathrm{F}^\partial} \int_f (\boldsymbol{\beta} \cdot \boldsymbol{n})^- p_D \, \mathsf{L}_{\mathcal{P}_{c_f}}(\mathsf{q}). \tag{2.8}$$

Alternative definitions resulting from the use of quadratures are discussed in section 4.2.

**Example 2.1** (Simplicial mesh). *Let us briefly discuss our scheme in the case of a sim-plicial mesh. Then, each mesh cell $c$ is a tetrahedron, see Figure 3. The tetrahedron $c$ is subdivided into 12 sub-tetrahedra composing the set $\mathfrak{P}_c$, and there are 6 internal subfaces in the set $\mathfrak{F}_c$ where the jump of the advective derivative is penalized; instead, this jump is not penalized on the four faces of $c$ (each composed of three subfaces). Obviously, standard stabilized finite element methods can be used on simplicial meshes as well.*
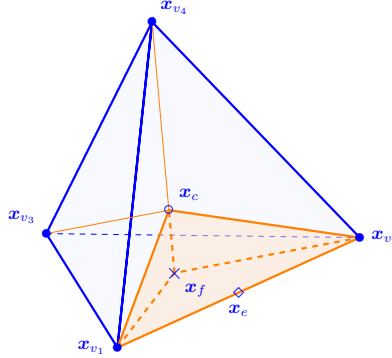


Figure 3: Tetrahedron $c$

## 3 Main results

This section contains our main results concerning the stability and error analysis of the discrete scheme (2.3); proofs are postponed to Section 5. To avoid the proliferation of constants in the analysis, we assume that $\gamma \in (\gamma_0, 1]$ with $\gamma_0 > 0$. We also assume that there are $0 < \rho_1 \leq \rho_2$ such that, for all $c \in \mathrm{C}$,

$$\rho_1 h_c |\boldsymbol{\beta}_c|^{-1} \leq \tau \leq \rho_2 \min\left(L_c^{-1}, \|\mu\|_{L^\infty(c)}^{-1}\right), \qquad (3.1)$$

with $L_c$ satisfying $\|\boldsymbol{\beta} - \boldsymbol{\beta}_c\|_{\boldsymbol{L}^\infty(c)} \leq L_c h_c$ and $\|\nabla \cdot \boldsymbol{\beta}\|_{L^\infty(c)} \leq L_c$. Notice that (3.1) implies $h_c |\boldsymbol{\beta}_c|^{-1} \max(L_c, \|\mu\|_{L^\infty(c)}) \leq \frac{\rho_2}{\rho_1}$, meaning that that the local mesh-size $h_c$ resolves the spatial variation of the vector field $\boldsymbol{\beta}$ and that we are not concerned with dominant reaction regimes. In what follows, we denote by $A \lesssim B$ the inequality $A \leq CB$ for positive real numbers $A, B, C$ where the value of $C$ can change at each occurrence, the value being independent of the mesh (as long as it satisfies (**M**)) and of the physical parameters (as long as (3.1) holds); the value of $C$ can depend on the time-scale $\tau$, and on the parameters $\rho_1$, $\rho_2$, and $\gamma_0$.

### 3.1 Properties of the reconstruction map

Let $c \in \mathrm{C}$. We equip the DoF space $\mathcal{P}_c$ with the following discrete norm:

$$\|\mathsf{p}\|_{2,c}^2 = h_c^3 \left(\mathsf{p}_c^2 + \sum_{v \in \mathrm{V}_c} \mathsf{p}_v^2\right), \qquad \forall \mathsf{p} \in \mathcal{P}_c. \qquad (3.2)$$

Under the mesh-regularity assumption (**M**), another, uniformly equivalent, choice for the discrete norm is $\|\mathsf{p}\|_{2,c}^2 = \frac{1}{2}\left(|c|\mathsf{p}_c^2 + \sum_{v \in \mathrm{V}_c} |\mathfrak{p}_{v,c}|\mathsf{p}_v^2\right)$.

6

**Lemma 3.1** (Stability). *Assume that the mesh satisfies (M). There exist $0 < C_\flat \leq C_\sharp$ such that*

$$C_\flat \|\mathsf{p}\|_{2,c}^2 \leq \|\mathsf{L}_{\mathcal{P}_c}(\mathsf{p})\|_{L^2(c)}^2 \leq C_\sharp \|\mathsf{p}\|_{2,c}^2, \tag{3.3}$$

*for all $\mathsf{p} \in \mathcal{P}_c$ and all $c \in \mathrm{C}$.*

Let us consider, for all $c \in \mathrm{C}$, the local reduction (or de Rham) map $\mathsf{R}_{\mathcal{P}_c} : \mathrm{D}(\mathsf{R}_{\mathcal{P}_c}) \to \mathcal{P}_c$ with domain $\mathrm{D}(\mathsf{R}_{\mathcal{P}_c}) := C^0(c)$ such that, for a continuous function $p : c \to \mathbb{R}$, the DoF vector $\mathsf{R}_{\mathcal{P}_c}(p) \in \mathcal{P}_c$ has components given by

$$(p(\boldsymbol{x}_v)_{v \in \mathrm{V}_c}, p(\boldsymbol{x}_c)).$$

Composing the reduction operator with the reconstruction map leads to the interpolation map $\mathcal{I}_{\mathcal{P}_c} = \mathsf{L}_{\mathcal{P}_c} \circ \mathsf{R}_{\mathcal{P}_c}$ mapping continuous functions in $c$ to continuous, piece-wise affine functions in $c$.

**Lemma 3.2** ($\mathbb{P}_1$-consistency). *For all $c \in \mathrm{C}$, affine polynomials in $c$ are left invariant by the interpolation map $\mathcal{I}_{\mathcal{P}_c}$, i.e.,*

$$\mathcal{I}_{\mathcal{P}_c}(P) = P, \qquad \forall P \in \mathbb{P}_1(c).$$

## 3.2 Well-posedness and inf-sup stability

We equip the global DoF space $\mathcal{P}$ with the following (so-called coercivity) norm:

$$\|\!|\mathsf{q}|\!\|^2 := \sum_{c \in \mathrm{C}} \left( \tau^{-1} \|\mathsf{q}\|_{2,c}^2 + \gamma_0 \, \mathsf{s}_c(\mathsf{q}, \mathsf{q}) \right) + \sum_{f \in \mathrm{F}^\partial} |\mathsf{q}|_f^2, \tag{3.4}$$

where $|\mathsf{q}|_f^2 := \frac{1}{2} \int_f |\boldsymbol{\beta} \cdot \boldsymbol{n}| \, \mathsf{L}_{\mathcal{P}_{c_f}}(\mathsf{q})^2$ (recall that $c_f$ is the unique mesh cell s.t. $f = \partial c \cap \partial \Omega$).

**Lemma 3.3** (Coercivity and well-posedness). *The following inequality holds:*

$$\mathsf{A}(\mathsf{p}, \mathsf{p}) + \mathsf{A}^\partial(\mathsf{p}, \mathsf{p}) \geq \|\!|\mathsf{p}|\!\|^2, \qquad \forall \mathsf{p} \in \mathcal{P}. \tag{3.5}$$

*Consequently, the discrete problem (2.3) is well-posed.*

The coercivity norm is not strong enough to establish an error estimate of order $\frac{3}{2}$. To this purpose, we show that inf-sup stability holds for the following stronger norm:

$$\|\!|\mathsf{q}|\!\|_\sharp^2 := \|\!|\mathsf{q}|\!\|^2 + \sum_{c \in \mathrm{C}} h_c |\boldsymbol{\beta}_c|^{-1} \|\boldsymbol{\beta}_c \cdot \nabla \mathsf{L}_{\mathcal{P}_c}(\mathsf{q})\|_{L^2(c)}^2. \tag{3.6}$$

**Lemma 3.4** (Inf-sup stability). *Assume that the mesh satisfies (M) and that assumption (3.1) holds. There exists $C_{\mathrm{STA}} > 0$ such that*

$$C_{\mathrm{STA}} \|\!|\mathsf{p}|\!\|_\sharp \leq \sup_{\mathsf{q} \in \mathcal{P} \backslash \{0\}} \frac{\mathsf{A}(\mathsf{p}, \mathsf{q}) + \mathsf{A}^\partial(\mathsf{p}, \mathsf{q})}{\|\!|\mathsf{q}|\!\|_\sharp}, \qquad \forall \mathsf{p} \in \mathcal{P}. \tag{3.7}$$

### 3.3 Bound on consistency error

To measure the consistency error for the discrete problem (2.3), we assume that the exact solution $p$ is in $H^s(\Omega)$, $s > \frac{3}{2}$, so that $p_{|c}$ is in the domain of $\mathsf{R}_{\mathcal{P}_c}$ for all $c \in \mathrm{C}$ and we can use the vector $\mathsf{R}_{\mathcal{P}_c}(p)$ to measure the consistency error locally. The global consistency error is defined such that

$$\mathcal{E}_{\mathrm{Cons}}(p) := \sup_{\mathsf{q} \in \mathcal{P}, \|\mathsf{q}\|_\sharp = 1} \left| \Xi(s, p_D; \mathsf{q}) - (\mathsf{A}(\mathsf{R}_{\mathcal{P}}(p), \mathsf{q}) + \mathsf{A}^\partial(\mathsf{R}_{\mathcal{P}}(p), \mathsf{q})) \right|, \tag{3.8}$$

where $\mathsf{R}_{\mathcal{P}}(p)$ is such that its restriction to a mesh cell $c \in \mathrm{C}$ is given by $\mathsf{R}_{\mathcal{P}_c}(p)$.

**Lemma 3.5** (Consistency). *Assume that the mesh satisfies (**M**) and that assumption (3.1) holds. Assume that $p \in H^2(\Omega)$. There exists $C_{\mathrm{Cons}} > 0$ such that*

$$\mathcal{E}_{\mathrm{Cons}}(p) \leq C_{\mathrm{Cons}} \left( \sum_{c \in \mathrm{C}} |\boldsymbol{\beta}_c| (h_c^{-1} \|p - \mathcal{I}_{\mathcal{P}_c}(p)\|_{L^2(c)}^2 + h_c |p - \mathcal{I}_{\mathcal{P}_c}(p)|_{H^1(c)}^2 + h_c^3 |p|_{H^2(c)}^2 \right)^{\frac{1}{2}}.$$

### 3.4 A priori error estimate

The last intermediate result we need before establishing our a priori error estimate is a bound on the interpolation error $p - \mathcal{I}_{\mathcal{P}_c}(p)$ for all $c \in \mathrm{C}$.

**Lemma 3.6** (Interpolation error). *Assume that the mesh satisfies (**M**). There exists $C_{\mathrm{Int}}$ such that*

$$\|p - \mathcal{I}_{\mathcal{P}_c}(p)\|_{L^2(c)} + h_c |p - \mathcal{I}_{\mathcal{P}_c}(p)|_{H^1(c)} \leq C_{\mathrm{Int}} h_c^2 |p|_{H^2(c)}, \tag{3.9}$$

*for all $p \in H^2(c)$ and all $c \in \mathrm{C}$.*

**Theorem 3.7** (Convergence rate). *Assume that the mesh satisfies (**M**) and that assumption (3.1) holds. Let $\mathsf{p} \in \mathcal{P}$ be the discrete solution of (2.3). Assume that the exact solution satisfies $p \in H^2(\Omega)$. There exists $C_{\mathrm{Conv}} > 0$ such that*

$$\|\mathsf{p} - \mathsf{R}_{\mathcal{P}}(p)\|_\sharp \leq C_{\mathrm{Conv}} \left( \sum_{c \in \mathrm{C}} |\boldsymbol{\beta}_c| h_c^3 |p|_{H^2(c)}^2 \right)^{\frac{1}{2}}.$$

*Proof.* Combine stability (Lemma 3.4), consistency (Lemma 3.5), and the approximation properties of the local interpolation maps $\mathcal{I}_{\mathcal{P}_c}(p)$ (Lemma 3.6). $\qquad\square$

## 4 Implementation aspects and numerical results

### 4.1 Elimination of cell-based unknowns

The algebraic realization of the discrete problem (2.3) is the linear system $\mathsf{Ap} = \Xi$ with $\mathsf{p} = (\mathsf{p}_\mathcal{V}, \mathsf{p}_\mathcal{C}) \in \mathcal{P}$,

$$\mathsf{A} = \begin{pmatrix} \mathsf{A}_{\mathcal{V}\mathcal{V}} & \mathsf{A}_{\mathcal{V}\mathcal{C}} \\ \mathsf{A}_{\mathcal{C}\mathcal{V}} & \mathsf{A}_{\mathcal{C}\mathcal{C}} \end{pmatrix} \quad \text{and} \quad \Xi = \begin{pmatrix} \Xi_\mathcal{V} \\ \Xi_\mathcal{C} \end{pmatrix}, \tag{4.1}$$

where $\Xi_\mathcal{X} \in \mathcal{X}$ is the restriction of $\Xi$ to $\mathcal{X}$ and $\mathsf{A}_{\mathcal{X}\mathcal{Y}} : \mathcal{Y} \to \mathcal{X}$ the restriction of $\mathsf{A}$ to $\mathcal{X}, \mathcal{Y}$ for $\mathcal{X}, \mathcal{Y} \in \{\mathcal{V}, \mathcal{C}\}$. Observing that $\mathsf{A}_{\mathcal{C}\mathcal{C}}$ is diagonal, one can easily compute its Schur complement so as to express $\mathsf{p}_\mathcal{C}$ in terms of $\mathsf{p}_\mathcal{V}$ and obtain a linear system in terms of $\mathsf{p}_\mathcal{V}$

only. This operation, which is often called static condensation in the finite element context, leads to the equivalent formulation $\widehat{\mathsf{A}}\mathsf{p} = \widehat{\Xi}$ where

$$\widehat{\mathsf{A}} = \begin{pmatrix} \mathsf{A}_{\mathcal{VV}} - \mathsf{A}_{\mathcal{VC}}\mathsf{A}_{\mathcal{CC}}^{-1}\mathsf{A}_{\mathcal{CV}} & \mathsf{0}_{\mathcal{CV}} \\ \mathsf{A}_{\mathcal{CC}}^{-1}\mathsf{A}_{\mathcal{CV}} & \mathsf{Id}_{\mathcal{CC}} \end{pmatrix} \quad \text{and} \quad \widehat{\Xi} = \begin{pmatrix} \Xi_{\mathcal{V}} - \mathsf{A}_{\mathcal{VC}}\mathsf{A}_{\mathcal{CC}}^{-1}\Xi_{\mathcal{C}} \\ \mathsf{A}_{\mathcal{CC}}^{-1}\Xi_{\mathcal{C}} \end{pmatrix}. \tag{4.2}$$

An interesting question is to compare the stencils associated with the blocks $\mathsf{A}_{\mathcal{VV}}$ and $\widehat{\mathsf{A}}_{\mathcal{VV}} = \mathsf{A}_{\mathcal{VV}} - \mathsf{A}_{\mathcal{VC}}\mathsf{A}_{\mathcal{CC}}^{-1}\mathsf{A}_{\mathcal{CV}}$. For all $v \in \mathrm{V}$, we introduce the sets

$$\mathsf{St}_{\mathrm{V}}(v) = \{v' \in \mathrm{V} \,|\, \mathsf{A}_{vv'} \neq 0\}, \quad \text{and} \quad \widehat{\mathsf{St}}_{\mathrm{V}}(v) = \{v' \in \mathrm{V} \,|\, \widehat{\mathsf{A}}_{vv'} \neq 0\}.$$

One can verify that $\widehat{\mathsf{St}}_{\mathrm{V}}(v) = \{v' \in \mathrm{V} \,|\, \mathrm{C}_v \cap \mathrm{C}_{v'} \neq \emptyset\}$ and that

$$\mathsf{St}_{\mathrm{V}}(v) = \widehat{\mathsf{St}}_{\mathrm{V}}(v) \cap \{v' \in \mathrm{V} \,|\, \exists v'' \in \mathrm{V}, \; \mathrm{F}_v \cap \mathrm{F}_{v''} \neq \emptyset \text{ and } \mathrm{F}_{v''} \cap \mathrm{F}_{v'} \neq \emptyset\},$$

so that $\mathsf{St}_{\mathrm{V}}(v) \subset \widehat{\mathsf{St}}_{\mathrm{V}}(v)$. The converse inclusion holds in the following situation.

**Lemma 4.1** (Vertex stencil). *Let $v \in \mathrm{V}$ and assume that for all $c \in \mathrm{C}_v$, all the vertices in $\mathrm{V}_c$ are connected to $v$ by a maximum of two faces of $c$, i.e., it is possible to find $f, f' \in \mathrm{F}_c$ with $f \cap f' \neq \emptyset$, $v \subset f$, and $v' \subset f'$ Then, $\mathsf{St}_{\mathrm{V}}(v) = \widehat{\mathsf{St}}_{\mathrm{V}}(v)$.*

*Proof.* Let $v' \in \widehat{\mathsf{St}}_{\mathrm{V}}(v)$. Reformulating the definition of $\widehat{\mathsf{St}}_{\mathrm{V}}(v)$ as $\{v' \in \mathrm{V} \,|\, \exists c \in \mathrm{C}_v, \; v' \in \mathrm{V}_c\}$, it follows, using the assumption, that there exist $f, f' \in \mathrm{F}_c$ with $f \cap f' \neq \emptyset$, $v \subset f$, and $v' \subset f'$. Denoting $v'' \in f \cap f'$, we obtain $\{v, v''\} \subset f$ and $\{v', v''\} \subset f'$, so that $\mathrm{F}_v \cap \mathrm{F}_{v''} \neq \emptyset$ and $\mathrm{F}_{v'} \cap \mathrm{F}_{v''} \neq \emptyset$. Hence, we infer that $v' \in \mathsf{St}_{\mathrm{V}}(v)$. $\square$

The assumption of Lemma 4.1 is often met in practice, as long as the mesh cells do not have too many vertices. An example of a cell that does not satisfy the assumption is shown in Figure 4.
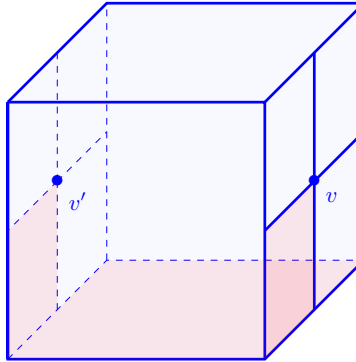


Figure 4: Example of cell (cf. CB sequence) which does not satisfy assumption of Lemma 4.1: $v$ and $v'$ are connected by at least 3 faces.

## 4.2 Numerical source term

Quadratures are often used in the computation of the source term (2.8) and the system matrix (2.5). For the system matrix, the considered advective fields allow for the use of exact quadratures. For the source term, we consider the approximation $\Xi^h$ given by

$$\Xi^h(s, p_D; \mathsf{q}) := \sum_{c \in \mathrm{C}} \int_c \mathcal{I}_{\mathcal{P}}(s)\, \mathsf{L}_{\mathcal{P}}(\mathsf{q}) + \sum_{f \in \mathrm{F}^\partial} \int_f (\boldsymbol{\beta}\cdot\boldsymbol{n})^- \mathcal{I}_{\mathcal{P}}(\widetilde{p_D})\, \mathsf{L}_{\mathcal{P}}(\mathsf{q}), \tag{4.3}$$

where $\widetilde{p_D}_{|f} = p_{D|f}$ for all $f \in F^\partial$; notice that $\mathcal{I}_\mathcal{P}(\widetilde{p_D})_{|f}$ is independent of the choice of the lifting $\widetilde{p_D}$ inside $\Omega$. The source term $\Xi^h$ has the advantage of being exactly computed using a second-order quadrature as soon as the boundary mesh is compatible with the inflow boundary $\partial\Omega^-$ (i.e., if the interior of a boundary face $f \in F^\partial$ intersects $\partial\Omega^-$, then $f \subset \partial\Omega^-$). However, using $\Xi^h$ in the discrete problem introduces an additional non-consistency, leading to the following additional term in the error bound:

$$\sup_{\mathsf{q}\in\mathcal{P}\setminus\{0\}} \frac{|(\Xi - \Xi^h)(s, p_D; \mathsf{q})|}{\|\|\mathsf{q}\|\|_\sharp}.$$

Then, the error estimate from Theorem 3.7 still holds with the following lemma.

**Lemma 4.2.** *Assume that the mesh satisfies (**M**) and that the mesh* M *is compatible with the inflow boundary $\partial\Omega^-$. Assume that $s \in H^2(C)$ and $p_D \in H^{3/2}(F^\partial)$. The following holds:*

$$\sup_{\mathsf{q}\in\mathcal{P}\setminus\{0\}} \frac{|(\Xi - \Xi^h)(s, p_D; \mathsf{q})|}{\|\|\mathsf{q}\|\|_\sharp} \lesssim \left( \sum_{c\in C} \tau h_c^4 \, |s|_{H^2(c)}^2 + \sum_{f\in F_c^\partial \cap \partial\Omega^-} |\boldsymbol{\beta}_{c_f}| h_{c_f}^3 \, |p_D|_{H^{3/2}(f)}^2 \right)^{\frac{1}{2}}.$$

## 4.3 Numerical illustration

The domain $\Omega$ is the unit cube $[0, 1]^3$ and we test three sequences of three-dimensional polyhedral meshes, each sequence consisting of successive uniform refinements of an initial mesh. The first sequence, denoted by H, consists of uniform hexahedral meshes, the second one, denoted by PrG, of prismatic meshes with polygonal basis, and the third one, denoted by CB, consists of checkerboard meshes with hanging nodes; see Figure 5. Notice that hanging nodes in the CB mesh sequence induce polyhedral cells composed of 26 vertices, 48 edges and 24 faces.
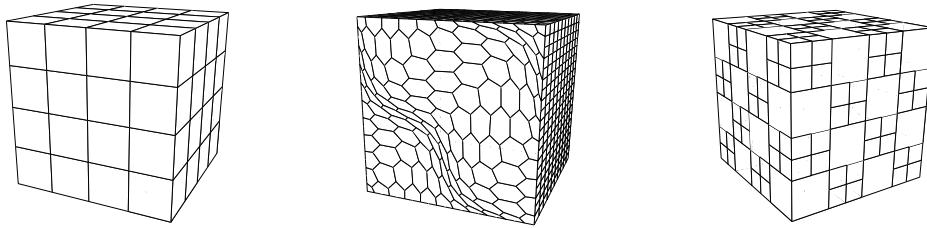


Figure 5: Examples of mesh from the three sequences. Left: hexahedral mesh; Middle: prismatic mesh with polygonal basis; Right: checkerboard mesh with hanging nodes.

### 4.3.1 Validation case : smooth solution

The exact solution $p$, the vector field $\boldsymbol{\beta}$ and the reaction term $\mu$ are given by

$$p(x, y, z) = \sin(\pi x)\sin(2\pi y)\sin(\pi z), \quad \boldsymbol{\beta} = \begin{pmatrix} y - 1/2 \\ 1/2 - x \\ z \end{pmatrix} \quad \text{and} \quad \mu = 1.$$

Notice that $p$ vanishes on the whole boundary $\partial\Omega$ and that $\mu - \frac{1}{2}\nabla\cdot\boldsymbol{\beta} = \frac{1}{2} > 0$. The stabilization parameter $\gamma$ in (2.5a) is equal to 0.01 (common optimal value for these three mesh sequences, see Section 4.3.2).

**Accuracy.** We perform a convergence study by computing the discrete $L^2$-error attached to vertex and cell DoFs, denoted by $\mathbf{Er}_{\mathcal{V}}(p)$ and $\mathbf{Er}_{\mathcal{C}}(p)$ respectively, and defined as

$$\mathbf{Er}_{\mathcal{V}}(p) := \left( \frac{\sum_{v \in V}(\mathsf{p}_v - \mathsf{R}_{\mathcal{P}}(p)_{|v})^2}{\sum_{v \in V}\mathsf{R}_{\mathcal{P}}(p)^2_{|v}} \right)^{\frac{1}{2}} \quad \text{and} \quad \mathbf{Er}_{\mathcal{C}}(p) := \left( \frac{\sum_{c \in C}(\mathsf{p}_c - \mathsf{R}_{\mathcal{P}}(p)_{|c})^2}{\sum_{c \in C}\mathsf{R}_{\mathcal{P}}(p)^2_c} \right)^{\frac{1}{2}}.$$

For these two error measures and for all the mesh sequences, the convergence rate is closer to 2 than to $\frac{3}{2}$ (see Figure 6); this type of behavior is often observed in practice. Moreover, the error attached to $\mathcal{C}$ seems to be less dependent on the type mesh. Moreover, the CB sequence leads to (slightly) smaller errors attached to $\mathcal{C}$ and to (slightly) larger errors attached to $\mathcal{V}$. One possible explanation is that for the CB sequence, the support of the reconstruction map attached to cells is more shape-regular than that attached to vertices.
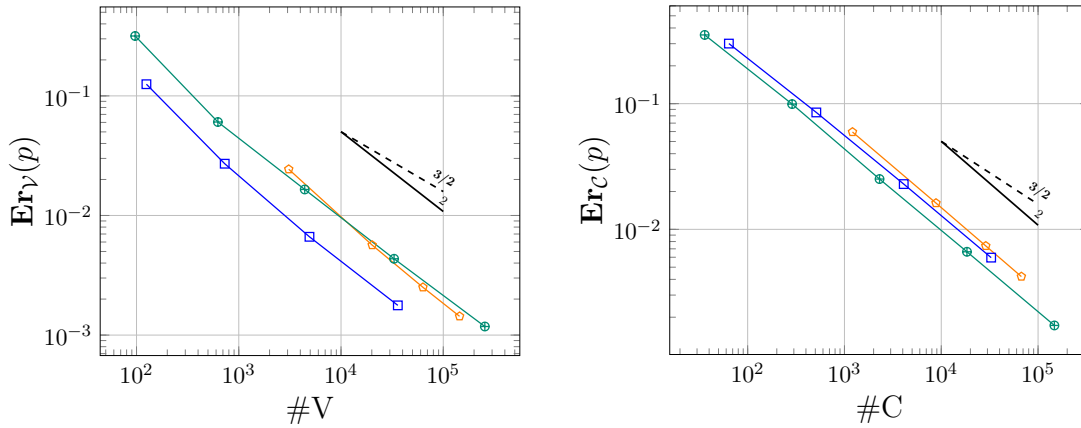


Figure 6: Discrete error $\mathbf{Er}_{\mathcal{V}}(p)$ (Left) and $\mathbf{Er}_{\mathcal{C}}(p)$ (Right) on H sequence (–□–), PrG sequence (–○–), and CB sequence (–⊕–).

**Cost.** We illustrate the advantage of the static condensation technique to eliminate locally cell DoFs. We compute the stockage benefit $\boldsymbol{\nu}$ and the speedup $\boldsymbol{\chi}$, defined by

$$\boldsymbol{\nu} = \frac{\text{NNZ}_{\text{nc}}}{\text{NNZ}_{\text{c}}} \quad \text{and} \quad \boldsymbol{\chi} = \frac{\boldsymbol{\chi}_{\text{nc}}}{\boldsymbol{\chi}_{\text{c}}},$$

where $\text{NNZ}_{\text{c}}$ and $\text{NNZ}_{\text{nc}}$ are the number of non-zero entries in the system matrix to invert with or without static condensation, respectively, and $\boldsymbol{\chi}_{\text{c}}$ and $\boldsymbol{\chi}_{\text{nc}}$ the computational costs defined by $\text{NNZ} \times \text{n}_{\text{ite}}$, where $\text{n}_{\text{ite}}$ is the number of iterations needed to bring the residual to a tolerance below $10^{-14}$, using a (diagonal) preconditioned bi-Conjugate Gradient Stabilized method. Results are reported in Tables 1, 2, and 3 for the three mesh sequences, respectively.

| #V | #V/#C | $\boldsymbol{\nu}$ | $\boldsymbol{\chi}$ | $\mathbf{Er}_{\mathcal{V}}(p)$ |
|---|---|---|---|---|
| 1.2e+02 | 1.95 | 1.50 | 2.78 | 1.3e-01 |
| 7.3e+02 | 1.42 | 1.56 | 3.18 | 2.7e-02 |
| 4.9e+03 | 1.20 | 1.59 | 3.67 | 6.6e-03 |
| 3.6e+04 | 1.10 | 1.61 | 3.48 | 1.8e-03 |

Table 1: Discrete error $\mathbf{Er}_{\mathcal{V}}(p)$, speedup $\boldsymbol{\chi}$, and ratio #V/#C on the H sequence.

| #V | #V/#C | $\nu$ | $\chi$ | $\mathbf{Er}_\mathcal{V}(p)$ |
|---|---|---|---|---|
| 3.1e+03 | 2.55 | 1.30 | 2.14 | 2.4e-02 |
| 2.0e+04 | 2.29 | 1.31 | 2.38 | 5.7e-03 |
| 6.3e+04 | 2.19 | 1.31 | 2.04 | 2.5e-03 |
| 1.4e+05 | 2.15 | 1.31 | 1.54 | 1.4e-03 |

Table 2: Discrete error $\mathbf{Er}_\mathcal{V}(p)$, speedup $\chi$, and ratio #V/#C on the `PrG` sequence.

| #V | #V/#C | $\nu$ | $\chi$ | $\mathbf{Er}_\mathcal{V}(p)$ |
|---|---|---|---|---|
| 9.7e+01 | 2.69 | 1.29 | 2.62 | 3.2e-01 |
| 6.2e+02 | 2.17 | 1.26 | 3.12 | 6.0e-02 |
| 4.4e+03 | 1.92 | 1.25 | 3.06 | 1.7e-02 |
| 3.3e+04 | 1.79 | 1.25 | 3.57 | 4.3e-03 |
| 2.5e+05 | 1.73 | 1.25 | 2.91 | 1.2e-03 |

Table 3: Discrete error $\mathbf{Er}_\mathcal{V}(p)$, speedup $\chi$, and ratio #V/#C on the `CB` sequence.

For these three sequences, we observe that the Schur complement method leads to a more competitive system regarding the stockage ($\nu > 1$) and the speedup ($\chi > 1$) criteria. Notice also that $\chi/\nu$ is proportional to the ratio of the condition number of these matrices, so that these results illustrate the fact that the condensed matrix is better conditionned. Notice also that the ratio $\nu$ is slightly smaller in Table 3 than in Table 2, reflecting the fact that the `CB` sequence does not satisfy the condition of Lemma 4.1, see also Figure 4, which leads to a slight increase of the stencil after static condensation.

### 4.3.2 Smooth solution with an internal layer

The exact solution $p$ is now given by

$$p(x,y,z) = xy \tanh\left( \frac{x}{2a} + \frac{y + z - \sqrt{2}}{a} \right), \qquad (4.4)$$

with $a = 0.05$, $\boldsymbol{\beta} = (1,1,0)$ and $\mu = 0$. We observe on Figure 7 that this potential present an internal layer around the plan $\frac{x}{2} + y + z = \sqrt{2}$.
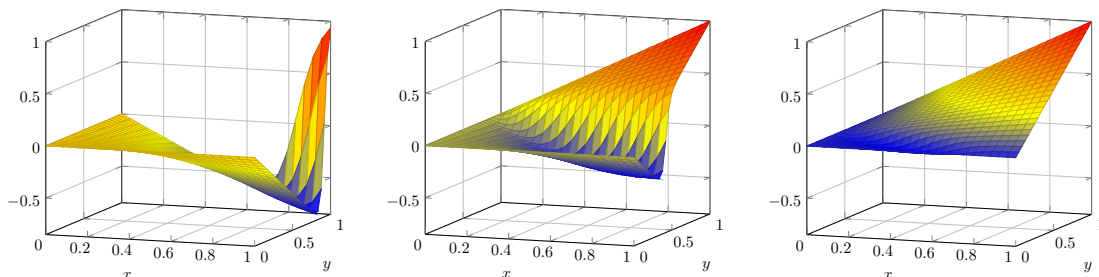


Figure 7: From left to right: exact solution $(x,y,z) \mapsto p(x,y,z)$ given by (4.4) for $z = 0$, $z = \frac{1}{2}$ and $z = 1$, respectively.

We report on Figures 8, 9 and 10 the error $\mathbf{Er}_\mathcal{V}(p)$ obtained for different values of the stabilization parameter $\gamma$. With no surprise, the error depends on the choice of this

parameter and the optimal value depends on the mesh sequence: among the tested values, $\gamma = 0.001$ is the best choice for the `PrG` sequence while $\gamma = 0.01$ works better for the `CB` sequence. To a lesser extent, this parameter also influences the convergence rate.
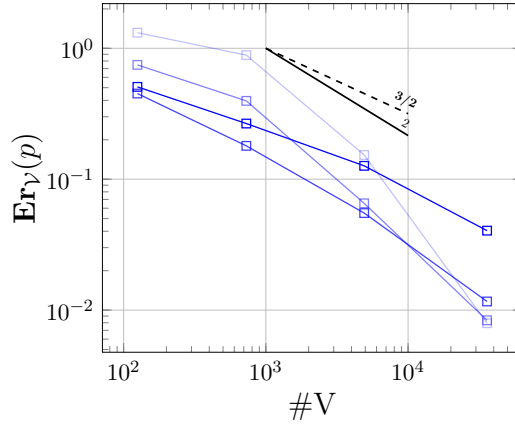


Figure 8: Discrete error $\mathbf{Er}_{\mathcal{V}}(p)$ with $\gamma = 0.001$ (⊟), $\gamma = 0.01$ (⊟), $\gamma = 0.1$ (⊟) and $\gamma = 1$ (⊟) .
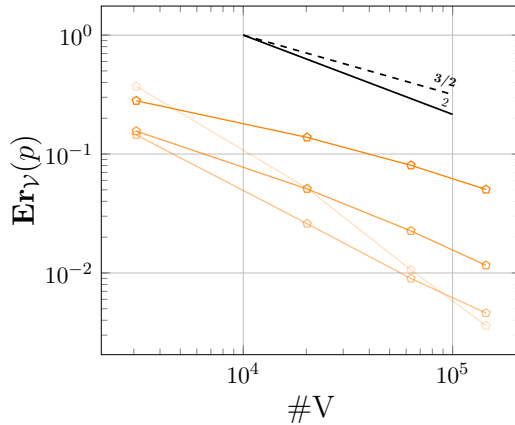


Figure 9: Discrete error $\mathbf{Er}_{\mathcal{V}}(p)$ with $\gamma = 0.001$ (⊙), $\gamma = 0.01$ (⊙), $\gamma = 0.1$ (⊙) and $\gamma = 1$ (⊙) .

## 5   Auxiliary results and proofs

This section collects the proofs of our main results stated in Section 3.

### 5.1   Auxiliary results on polyhedral cells

**Lemma 5.1** (Inverse inequality). *Assume that the mesh satisfies (**M**). There exists $C_{\text{INV}} > 0$ such that*

$$|q|_{H^1(\mathfrak{p})} \leq C_{\text{INV}} h_c^{-1} \|q\|_{L^2(\mathfrak{p})}, \tag{5.1}$$

*for all $q$ continuous and piece-wise affine in $c$, all $\mathfrak{p} \in \mathfrak{P}_c$, and all $c \in \mathrm{C}$.*
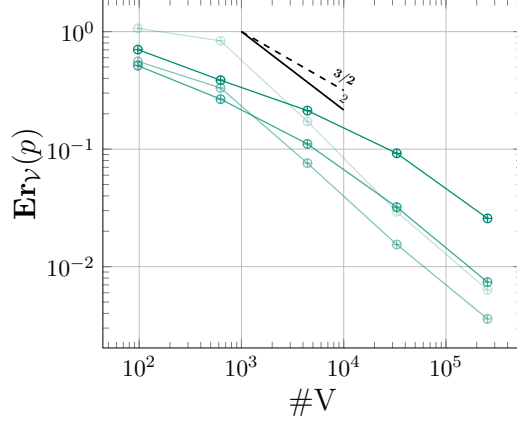
*Proof.* See [12, Lemma 1.44]. □

Figure 10: Discrete error $\mathbf{Er}_{\mathcal{V}}(p)$ with $\gamma = 0.001$ ($\!-\!\oplus\!-\!$), $\gamma = 0.01$ ($\!-\!\oplus\!-\!$), $\gamma = 0.1$ ($\!-\!\oplus\!-\!$) and $\gamma = 1$ ($\!-\!\oplus\!-\!$) .

**Lemma 5.2** (Multiplicative trace inequality). *Assume that the mesh satisfies (**M**). Let $c \in \mathrm{C}$. There exists $C_\mathrm{T} > 0$ such that*

$$\|q\|_{L^2(\mathfrak{f})}^2 \le C_\mathrm{T} \|q\|_{L^2(\mathfrak{p})} (h_c^{-1} \|q\|_{L^2(\mathfrak{p})} + |q|_{H^1(\mathfrak{p})}), \tag{5.2}$$

*for all $q \in H^1(\mathfrak{p})$, all $\mathfrak{p} \subset \mathfrak{P}_c$, all $\mathfrak{f} \in \mathfrak{F}_c$ such that $\mathfrak{f} \subset \partial\mathfrak{p}$, and all $c \in \mathrm{C}$.*

*Proof.* See [12, Lemma 1.49]. $\qquad\square$

**Lemma 5.3** (Polynomial approximation). *Assume that the mesh satisfies (**M**). There exists $C_{\mathrm{Pol}} > 0$ such that*

$$\inf_{P \in \mathbb{P}_1(c)} (\|p - P\|_{L^2(c)} + h_c |p - P|_{H^1(c)}) \le C_{\mathrm{Pol}} h_c^2 |p|_{H^2(c)}, \tag{5.3}$$

*for all $p \in H^2(c)$ and all $c \in \mathrm{C}$.*

*Proof.* We follow the ideas in [15]. Since the partition $\mathfrak{P}_c$ consists of a finite number of tetrahedra connected through their faces, we can proceed as in [15, Lemma 5.5] to infer that there exists $C_{\mathrm{PS}} > 0$ such that the following so-called local Poincaré(–Steklov) inequality holds:

$$\|q - \overline{q}^c\|_{L^2(c)} \le C_{\mathrm{PS}} h_c |q|_{H^1(c)},$$

for all $q \in H^1(c)$ with $\overline{q}^c := \frac{1}{|c|} \int_c q$ and all $c \in \mathrm{C}$. Notice that whenever the mesh cell $c$ is a convex set, one can take $C_{\mathrm{PS}} = \pi^{-1}$, see [2]. Let now $p \in H^2(c)$ and $c \in \mathrm{C}$. Let us consider the affine polynomial $P(\boldsymbol{x}) := \overline{p}^c + \overline{\nabla p}^c \cdot (\boldsymbol{x} - \boldsymbol{x}_c)$. Then, applying the Poincaré inequality component-wise, we first infer that

$$|p - P|_{H^1(c)} = \|\nabla p - \overline{\nabla p}^c\|_{L^2(c)} \le C_{\mathrm{PS}} h_c |\nabla p|_{\boldsymbol{H}^1(c)} \le 2 C_{\mathrm{PS}} h_c |p|_{H^2(c)},$$

since cross-derivatives are counted only once in the $H^2$-seminorm. Moreover, since the function $p - P$ has zero mean-value in $c$ by construction, applying again the Poincaré inequality, we infer that

$$\|p - P\|_{L^2(c)} \le C_{\mathrm{PS}} h_c |p - P|_{H^1(c)} \le 2 C_{\mathrm{PS}}^2 h_c^2 |p|_{H^2(c)},$$

owing to the above bound on $|p - P|_{H^1(c)}$. $\qquad\square$

## 5.2 Properties of the local reconstruction map

*Proof of Lemma 3.1.* Let $c \in C$. Given real numbers $(\lambda_v)_{v \in V_c}$, $(\lambda_f)_{f \in F_c}$, and $\lambda_c$, it is well-known (see, e.g., [13, §9.1.3]) from the spectral properties of the mass matrix of $\mathbb{P}_1$ Lagrange finite elements that the assumption on mesh regularity implies that there are uniform constants $0 < C_1 \leq C_2$ such that the function $f_\lambda := \sum_{v \in V_c} \lambda_v \theta_v + \sum_{f \in F_c} \lambda_f \theta_f + \lambda_c \theta_c$ satisfies

$$C_1 \|\lambda\|_{\ell^2}^2 \leq h_c^{-3} \|f_\lambda\|_{L^2(c)}^2 \leq C_2 \|\lambda\|_{\ell^2}^2, \tag{5.4}$$

with $\|\lambda\|_{\ell^2}^2 = \sum_{v \in V_c} |\lambda_v|^2 + \sum_{f \in F_c} |\lambda_f|^2 + |\lambda_c|^2$. Consider now $\mathsf{p} \in \mathcal{P}_c$ and observe that

$$\mathsf{L}_{\mathcal{P}_c}(\mathsf{p}) = \sum_{v \in V_c} \mathsf{p}_v \theta_v + \sum_{f \in F_c} \left( \sum_{v \in V_f} \omega_{v,f} \mathsf{p}_v \right) \theta_f + \mathsf{p}_c \theta_c,$$

where $\omega_{v,f} := \frac{|f \cap \mathsf{p}_{v,c}|}{|f|}$ satisfies $\omega_{v,f} \in (0,1)$. Applying the lower bound in (5.4) to $f_\lambda = \mathsf{L}_{\mathcal{P}_c}(\mathsf{p})$, we infer that the lower bound in (3.3) holds with $C_\flat = C_1$. Applying now the upper bound in (5.4) and observing that

$$\sum_{f \in F_c} \left| \sum_{v \in V_f} \omega_{v,f,c} \mathsf{p}_v \right|^2 \leq \sum_{f \in F_c} \sum_{v \in V_f} \#V_f |\mathsf{p}_v|^2 = \sum_{v \in V_c} \left( \sum_{f \in F_v \cap F_c} \#V_f \right) |\mathsf{p}_v|^2,$$

the upper bound in (3.3) holds with $C_\sharp = C_2(1 + \max_{v \in V_c} \sum_{f \in F_v \cap F_c} \#V_f)$. $\qquad\square$

*Proof of Lemma 3.2.* Let $c \in C$. Let $P \in \mathbb{P}_1(c)$ with $P(\boldsymbol{x}) = \boldsymbol{a} \cdot \boldsymbol{x} + b$ and $(\boldsymbol{a}, b) \in \mathbb{R}^3 \times \mathbb{R}$. We observe that

$$\mathsf{L}_{\mathcal{P}_c} \mathsf{R}_{\mathcal{P}_c}(P)(\boldsymbol{x}) = \sum_{v \in V_c} (\boldsymbol{a} \cdot \boldsymbol{x}_v + b) \ell_{v,c}(\boldsymbol{x}) + (\boldsymbol{a} \cdot \boldsymbol{x}_c + b) \ell_c(\boldsymbol{x})$$

$$= \boldsymbol{a} \cdot \left( \sum_{v \in V_c} \boldsymbol{x}_v \ell_{v,c}(\boldsymbol{x}) + \boldsymbol{x}_c \ell_c(\boldsymbol{x}) \right) + \left( \sum_{v \in V_c} \ell_{v,c}(\boldsymbol{x}) + \ell_c(\boldsymbol{x}) \right) b.$$

Recalling that $\omega_{v,f} := \frac{|f \cap \mathsf{p}_{v,c}|}{|f|}$ and using the definition of the local reconstruction functions and the properties of the Courant basis functions, we infer that

$$\sum_{v \in V_c} \ell_{v,c}(\boldsymbol{x}) + \ell_c(\boldsymbol{x}) = \sum_{v \in V_c} \theta_v(\boldsymbol{x}) + \sum_{f \in F_c} \left( \sum_{v \in V_f} \omega_{v,f} \right) \theta_f(\boldsymbol{x}) + \theta_c(\boldsymbol{x})$$

$$= \sum_{v \in V_c} \theta_v(\boldsymbol{x}) + \sum_{f \in F_c} \theta_f(\boldsymbol{x}) + \theta_c(\boldsymbol{x}) \equiv 1,$$

and

$$\sum_{v \in V_c} \boldsymbol{x}_v \ell_{v,c}(\boldsymbol{x}) + \boldsymbol{x}_c \ell_c(\boldsymbol{x}) = \sum_{v \in V_c} \boldsymbol{x}_v \theta_v(\boldsymbol{x}) + \sum_{f \in F_c} \left( \sum_{v \in V_f} \omega_{v,f} \boldsymbol{x}_v \right) \theta_f(\boldsymbol{x}) + \boldsymbol{x}_c \theta_c(\boldsymbol{x})$$

$$= \sum_{v \in V_c} \boldsymbol{x}_v \theta_v(\boldsymbol{x}) + \sum_{f \in F_c} \boldsymbol{x}_f \theta_f(\boldsymbol{x}) + \boldsymbol{x}_c \theta_c(\boldsymbol{x}) \equiv \boldsymbol{x},$$

since $\sum_{v \in V_f} \omega_{v,f} = 1$ and $\sum_{v \in V_f} \omega_{v,f} \boldsymbol{x}_v = \boldsymbol{x}_f$ (see [4, Proposition 5.23]). $\qquad\square$

### 5.3 Well-posedness and inf-sup stability

*Proof of Lemma 3.3.* Let $c \in C$. Let $\mathsf{p} \in \mathcal{P}_c$. Applying the Leibniz rule to integrate by parts the advective derivative (recall that $\mathsf{L}_{\mathcal{P}_c}(\mathsf{p})$ is a continuous function in $c$), we infer that

$$\mathsf{A}_c(\mathsf{p}, \mathsf{p}) \geq \tau^{-1} \|\mathsf{p}\|_{2,c}^2 + \gamma_0 \mathsf{s}_c(\mathsf{p}, \mathsf{p}) + \frac{1}{2} \int_c \nabla \cdot (\boldsymbol{\beta} \, \mathsf{L}_{\mathcal{P}_c}(\mathsf{p})^2).$$

Let now $\mathsf{p} \in \mathcal{P}$. For all the mesh faces $f \in F$ such that $f = \partial c_1 \cap \partial c_2$, we have $\mathsf{L}_{\mathcal{P}_{c_1}}(\mathsf{p})_{|f} = \mathsf{L}_{\mathcal{P}_{c_2}}(\mathsf{p})_{|f}$ (since these two functions are uniquely determined by the DoFs of $\mathsf{p}$ at the vertices $v \in V_f$). Then, summing the above relation for all $c \in C$ and using the divergence theorem, we infer that

$$\sum_{c \in C} \mathsf{A}_c(\mathsf{p}, \mathsf{p}) \geq \sum_{c \in C} \left( \tau^{-1} \|\mathsf{p}\|_{2,c}^2 + \gamma_0 \mathsf{s}_c(\mathsf{p}, \mathsf{p}) \right) + \sum_{c \in C} \frac{1}{2} \int_c \nabla \cdot (\boldsymbol{\beta} \, \mathsf{L}_{\mathcal{P}_c}(\mathsf{p})^2)$$

$$= \sum_{c \in C} \left( \tau^{-1} \|\mathsf{p}\|_{2,c}^2 + \gamma_0 \mathsf{s}_c(\mathsf{p}, \mathsf{p}) \right) + \sum_{f \in F^\partial} \frac{1}{2} \int_f (\boldsymbol{\beta} \cdot \boldsymbol{n}) \mathsf{L}_{\mathcal{P}_{c_f}}(\mathsf{p})^2.$$

Finally, (3.5) follows by combining the last term with the term $\mathsf{A}^\partial(\mathsf{p}, \mathsf{p})$. $\qquad \square$

*Proof of Lemma 3.4.* Let $\mathsf{p} \in \mathcal{P}$ and let us set $S := \sup_{\mathsf{q} \in \mathcal{P} \setminus \{0\}} \frac{\mathsf{A}(\mathsf{p}, \mathsf{q}) + \mathsf{A}^\partial(\mathsf{p}, \mathsf{q})}{\|\mathsf{q}\|_\sharp}$. Lemma 3.3 implies that

$$\|\mathsf{p}\|^2 \leq \mathsf{A}(\mathsf{p}, \mathsf{p}) + \mathsf{A}^\partial(\mathsf{p}, \mathsf{p}) \leq S \|\mathsf{p}\|_\sharp.$$

It remains to control the advective derivative. Let us define $\mathsf{q} \in \mathcal{P}$ such that $\mathsf{q}_v = 0$ for all $v \in V$ and, for all $c \in C$,

$$\mathsf{q}_c := h_c |\boldsymbol{\beta}_c|^{-1} \frac{1}{\# \mathfrak{P}_c} \sum_{\mathfrak{p} \in \mathfrak{P}_c} \boldsymbol{\beta}_c \cdot \nabla \mathsf{L}_{\mathcal{P}_c}(\mathsf{p})_{|\mathfrak{p}},$$

recalling that $\mathsf{L}_{\mathcal{P}_c}(\mathsf{p})$ is a piece-wise affine function on the partition of $c$ induced by $\mathfrak{P}_c$. Let us first notice that

$$h_c^{-1} |\boldsymbol{\beta}_c| \|\mathsf{q}\|_{2,c}^2 = h_c^2 |\boldsymbol{\beta}_c| \mathsf{q}_c^2 \leq h_c^4 |\boldsymbol{\beta}_c|^{-1} \frac{1}{\# \mathfrak{P}_c} \sum_{\mathfrak{p} \in \mathfrak{P}_c} |\boldsymbol{\beta}_c \cdot \nabla \mathsf{L}_{\mathcal{P}_c}(\mathsf{p})_{|\mathfrak{p}}|^2$$

$$\lesssim h_c |\boldsymbol{\beta}_c|^{-1} \|\boldsymbol{\beta}_c \cdot \nabla \mathsf{L}_{\mathcal{P}_c}(\mathsf{p})\|_{L^2(c)}^2.$$

Observing that $|\mathsf{q}|_f = 0$ for all $f \in F^\partial$ since $\mathsf{L}_{\mathcal{P}_c}(\mathsf{q})$ vanishes on the boundary $\partial c$ for all $c \in C$, we infer that $\|\mathsf{q}\|_\sharp^2 = \sum_{c \in C} (\tau^{-1} \|\mathsf{q}\|_{2,c}^2 + \gamma_0 \mathsf{s}_c(\mathsf{q}, \mathsf{q}) + h_c |\boldsymbol{\beta}_c|^{-1} \|\boldsymbol{\beta}_c \cdot \nabla \mathsf{L}_{\mathcal{P}_c}(\mathsf{q})\|_{L^2(c)}^2)$ and obtain the following bounds:

$$\tau^{-1} \|\mathsf{q}\|_{2,c}^2 \leq \rho_1^{-1} h_c^{-1} |\boldsymbol{\beta}_c| \|\mathsf{q}\|_{2,c}^2 \lesssim h_c |\boldsymbol{\beta}_c|^{-1} \|\boldsymbol{\beta}_c \cdot \nabla \mathsf{L}_{\mathcal{P}_c}(\mathsf{p})\|_{L^2(c)}^2,$$

$$\gamma_0 \mathsf{s}_c(\mathsf{q}, \mathsf{q}) \lesssim h_c |\boldsymbol{\beta}_c|^{-1} \|\boldsymbol{\beta}_c \cdot \nabla \mathsf{L}_{\mathcal{P}_c}(\mathsf{p})\|_{L^2(c)}^2,$$

$$h_c |\boldsymbol{\beta}_c|^{-1} \|\boldsymbol{\beta}_c \cdot \nabla \mathsf{L}_{\mathcal{P}_c}(\mathsf{q})\|_{L^2(c)}^2 \leq C_{\text{Inv}}^2 C_\sharp h_c^{-1} |\boldsymbol{\beta}_c| \|\mathsf{q}\|_{2,c}^2 \leq C h_c |\boldsymbol{\beta}_c|^{-1} \|\boldsymbol{\beta}_c \cdot \nabla \mathsf{L}_{\mathcal{P}_c}(\mathsf{p})\|_{L^2(c)}^2,$$

owing to (3.1) for the first line, $\gamma_0 \leq 1$, Lemma 5.2, and the definition of $\mathsf{s}_c$ for the second line, and owing to the inverse inequality (5.1) and Lemma 3.1 for the third line. Collecting these bounds, we obtain

$$\|\mathsf{q}\|_\sharp^2 \lesssim \sum_{c \in C} h_c |\boldsymbol{\beta}_c|^{-1} \|\boldsymbol{\beta}_c \cdot \nabla \mathsf{L}_{\mathcal{P}_c}(\mathsf{p})\|_{L^2(c)}^2 \lesssim \|\mathsf{p}\|_\sharp^2.$$

Using the inverse inequality $C_\theta^{-1}\|\phi\|_{L^2(c)}^2 \le \int_c \theta_c \phi^2$, valid for any piece-wise affine function $\phi$ in $c$, we infer that

$$C_\theta^{-1} h_c |\boldsymbol{\beta}_c|^{-1} \|\boldsymbol{\beta}_c \cdot \nabla \mathsf{L}_{\mathcal{P}_c}(\mathsf{p})\|_{L^2(c)}^2 \le \int_c (\boldsymbol{\beta}_c \cdot \nabla \mathsf{L}_{\mathcal{P}_c}(\mathsf{p}))(h_c|\boldsymbol{\beta}_c|^{-1}\theta_c \boldsymbol{\beta}_c \cdot \nabla \mathsf{L}_{\mathcal{P}_c}(\mathsf{p}))$$

$$= \int_c (\boldsymbol{\beta}_c \cdot \nabla \mathsf{L}_{\mathcal{P}_c}(\mathsf{p}))\mathsf{L}_{\mathcal{P}_c}(\mathsf{q}) + \Delta_c,$$

with

$$\Delta_c = h_c|\boldsymbol{\beta}_c|^{-1}\int_c (\boldsymbol{\beta}_c \cdot \nabla \mathsf{L}_{\mathcal{P}_c}(\mathsf{p}))\theta_c \left( \boldsymbol{\beta}_c \cdot \nabla \mathsf{L}_{\mathcal{P}_c}(\mathsf{p}) - \frac{1}{\#\mathfrak{P}_c} \sum_{\mathfrak{p} \in \mathfrak{P}_c} \boldsymbol{\beta}_c \cdot \nabla \mathsf{L}_{\mathcal{P}_c}(\mathsf{p})_{|\mathfrak{p}} \right),$$

where we have used that $\mathsf{L}_{\mathcal{P}_c}(\mathsf{q}) = \mathsf{q}_c \theta_c$ and the definition of $\mathsf{q}_c$. Owing to the bound (see, e.g., [1, 8, 15])

$$h_c|\boldsymbol{\beta}_c|^{-1}\left\| \boldsymbol{\beta}_c \cdot \nabla \mathsf{L}_{\mathcal{P}_c}(\mathsf{p}) - \frac{1}{\#\mathfrak{P}_c}\sum_{\mathfrak{p}\in\mathfrak{P}_c} \boldsymbol{\beta}_c \cdot \nabla \mathsf{L}_{\mathcal{P}_c}(\mathsf{p})_{|\mathfrak{p}} \right\|_{L^2(c)}^2 \le C_{\mathrm{Avg}}\mathsf{s}_c(\mathsf{p},\mathsf{p}),$$

we can use the Cauchy–Schwarz inequality, $\theta_c \le 1$, and Young's inequality to bound $\Delta_c$, and infer that

$$(2C_\theta)^{-1}h_c|\boldsymbol{\beta}_c|^{-1}\|\boldsymbol{\beta}_c \cdot \nabla \mathsf{L}_{\mathcal{P}_c}(\mathsf{p})\|_{L^2(c)}^2 \le \int_c (\boldsymbol{\beta}_c \cdot \nabla \mathsf{L}_{\mathcal{P}_c}(\mathsf{p}))\mathsf{L}_{\mathcal{P}_c}(\mathsf{q}) + \frac{1}{2}C_\theta C_{\mathrm{Avg}}\mathsf{s}_c(\mathsf{p},\mathsf{p}).$$

We next observe that

$$\int_c (\boldsymbol{\beta}_c \cdot \nabla \mathsf{L}_{\mathcal{P}_c}(\mathsf{p}))\mathsf{L}_{\mathcal{P}_c}(\mathsf{q}) = \mathsf{A}_c(\mathsf{p},\mathsf{q}) - \Delta_c',$$

with

$$\Delta_c' = \int_c \mu \mathsf{L}_{\mathcal{P}_c}(\mathsf{p})\mathsf{L}_{\mathcal{P}_c}(\mathsf{q}) + \int_c ((\boldsymbol{\beta} - \boldsymbol{\beta}_c)\cdot \nabla \mathsf{L}_{\mathcal{P}_c}(\mathsf{p}))\mathsf{L}_{\mathcal{P}_c}(\mathsf{q}) + \gamma \mathsf{s}_c(\mathsf{p},\mathsf{q}).$$

Using (3.1), the inverse inequality (5.1), and Lemma 3.1 together with the Cauchy–Schwarz inequality, we infer that

$$\sum_{c \in \mathrm{C}} |\Delta_c'| \lesssim \|\!|\mathsf{p}|\!\|\,\|\!|\mathsf{q}|\!\|.$$

Collecting the above bounds, we infer that

$$\sum_{c\in\mathrm{C}} h_c|\boldsymbol{\beta}_c|^{-1}\|\boldsymbol{\beta}_c\cdot\nabla\mathsf{L}_{\mathcal{P}_c}(\mathsf{p})\|_{L^2(c)}^2 \lesssim \sum_{c\in\mathrm{C}}\mathsf{A}_c(\mathsf{p},\mathsf{q}) + \|\!|\mathsf{p}|\!\|\,\|\mathsf{p}\|_\sharp.$$

Finally, since $\sum_{c\in\mathrm{C}}\mathsf{A}_c(\mathsf{p},\mathsf{q}) = \mathsf{A}(\mathsf{p},\mathsf{q}) = \mathsf{A}(\mathsf{p},\mathsf{q}) + \mathsf{A}^\partial(\mathsf{p},\mathsf{q}) \le S\|\mathsf{q}\|_\sharp \lesssim S\|\mathsf{p}\|_\sharp$, we finally obtain

$$\|\mathsf{p}\|_\sharp^2 \lesssim S\|\mathsf{p}\|_\sharp + \|\!|\mathsf{p}|\!\|\,\|\mathsf{p}\|_\sharp,$$

whence the conclusion follows from $\|\!|\mathsf{p}|\!\|^2 \le S\|\mathsf{p}\|_\sharp$ and Young's inequality. $\qquad\square$

### 5.4 Bound on consistency error

*Proof of Lemma 3.5.* Let us set $y_c = p - \mathcal{I}_{\mathcal{P}_c}(p)$ for all $c \in \mathrm{C}$. Recalling the properties of the exact solution and the definition (2.8) of the linear form $\Xi$ and the local definitions (2.5) and (2.7) of the bilinear forms $\mathsf{A}_c$ and $\mathsf{A}_f^\partial$ for all $c \in \mathrm{C}$ and all $f \in \mathrm{F}^\partial$, respectively, we infer that

$$\Xi(s, p_D; \mathsf{q}) - (\mathsf{A}(\mathsf{R}_{\mathcal{P}}(p), \mathsf{q}) + \mathsf{A}^\partial(\mathsf{R}_{\mathcal{P}}(p), \mathsf{q})) = T_1 + T_2 + T_3,$$

where

$$T_1 := \sum_{c \in \mathrm{C}} - \int_c y_c \left( \boldsymbol{\beta}_c \cdot \nabla \mathsf{L}_{\mathcal{P}_c}(\mathsf{q}) + (\boldsymbol{\beta} - \boldsymbol{\beta}_c) \cdot \nabla \mathsf{L}_{\mathcal{P}_c}(\mathsf{q}) - (\mu - \nabla \cdot \boldsymbol{\beta}) \, \mathsf{L}_{\mathcal{P}_c}(\mathsf{q}) \right),$$

$$T_2 := \sum_{c \in \mathrm{C}} \gamma h_c^2 |\boldsymbol{\beta}_c|^{-1} \sum_{\mathfrak{f} \in \mathfrak{F}_c} \int_{\mathfrak{f}} (\boldsymbol{\beta}_c \cdot [\![\nabla y_c]\!])(\boldsymbol{\beta}_c \cdot [\![\nabla \mathsf{L}_{\mathcal{P}_c}(\mathsf{q})]\!]),$$

$$T_3 := \sum_{f \in \mathrm{F}^\partial} \int_f (\boldsymbol{\beta} \cdot \boldsymbol{n})^+ y_{c_f} \, \mathsf{L}_{\mathcal{P}_{c_f}}(\mathsf{q}),$$

where we have used that

$$\sum_{c \in \mathrm{C}} \int_c (\boldsymbol{\beta} \cdot \nabla y_c) \mathsf{L}_{\mathcal{P}_c}(\mathsf{q}) = \sum_{c \in \mathrm{C}} - \int_c y_c \left( \boldsymbol{\beta} \cdot \nabla \mathsf{L}_{\mathcal{P}_c}(\mathsf{q}) + (\nabla \cdot \boldsymbol{\beta}) \mathsf{L}_{\mathcal{P}_c}(\mathsf{q}) \right) + \sum_{f \in \mathrm{F}^\partial} \int_f (\boldsymbol{\beta} \cdot \boldsymbol{n}) y_{c_f} \mathsf{L}_{\mathcal{P}_{c_f}}(\mathsf{q})$$

in the evaluation of $T_1$, the fact that $[\![\nabla p]\!]_{|\mathfrak{f}} = 0$ for all $\mathfrak{f} \in \mathfrak{F}_c$ in the evaluation of $T_2$, and the fact that $p_D = p_{|\partial \Omega}$ in the evaluation of $T_3$. Applying now the Cauchy-Schwarz inequality, Lemma 5.1, and recalling that $\boldsymbol{\beta}$ is Lipschitz, we infer that

$$|T_1| \lesssim \left( \sum_{c \in \mathrm{C}} (|\boldsymbol{\beta}_c| h_c^{-1} + (L_c C_{\mathrm{INV}} C_\sharp)^2 \tau + (\|\mu - \nabla \cdot \boldsymbol{\beta}\|_{L^\infty(c)} C_\sharp)^2 \tau) \|y_c\|_{L^2(c)}^2 \right)^{\frac{1}{2}} \| \mathsf{q} \|_\sharp$$

so that assumption (3.1) implies that

$$|T_1| \lesssim \left( \sum_{c \in \mathrm{C}} |\boldsymbol{\beta}_c| h_c^{-1} \|y_c\|_{L^2(c)}^2 \right)^{\frac{1}{2}} \| \mathsf{q} \|_\sharp.$$

Furthermore, using the multiplicative trace inequality from Lemma 5.2, we infer that

$$|T_2| \lesssim \left( \sum_{c \in \mathrm{C}} \sum_{\mathfrak{f} \in \mathfrak{F}_c} h_c^2 |\boldsymbol{\beta}_c|^{-1} \|\boldsymbol{\beta}_c \cdot [\![\nabla y_c]\!]\|_{L^2(\mathfrak{f})}^2 \right)^{\frac{1}{2}} \| \mathsf{q} \|_\sharp$$

$$\lesssim \left( \sum_{c \in \mathrm{C}} |\boldsymbol{\beta}_c| (h_c |y_c|_{H^1(c)}^2 + h_c^3 |p|_{H^2(c)}^2) \right)^{\frac{1}{2}} \| \mathsf{q} \|_\sharp.$$

Finally, still using Lemma 5.2, this time for each face $f \in \mathrm{F}^\partial$ and the corresponding mesh cell $c_f$, we infer that

$$|T_3| \lesssim \left( \sum_{f \in \mathrm{F}^\partial} |\boldsymbol{\beta}_{c_f}| (h_{c_f}^{-1} \|y_{c_f}\|_{L^2(c_f)}^2 + h_{c_f} |y_{c_f}|_{H^1(c_f)}^2) \right)^{\frac{1}{2}} \| \mathsf{q} \|_\sharp.$$

Collecting these bounds leads to the assertion. $\qquad\qquad \square$

## 5.5 A priori error estimate

*Proof of Lemma 3.6.* Let us first prove that there exists $C_\mathsf{R}$ such that

$$\|\mathsf{R}_{\mathcal{P}_c}(p)\|_{2,c} \le C_\mathsf{R} \left( \|p\|_{L^2(c)} + h_c |p|_{H^1(c)} + h_c^2 |p|_{H^2(c)} \right), \tag{5.5}$$

for all $p \in H^2(c)$ and all $c \in \mathrm{C}$. Consider a tetrahedron $\mathfrak{p} \in \mathfrak{P}_c$. Proceeding as for finite element proofs (using a reference tetrahedron and the continuous embedding $H^2(\mathfrak{p}) \hookrightarrow L^\infty(\mathfrak{p})$; see, e.g., [13, §1.5]), we infer using mesh regularity that

$$\|p\|_{L^\infty(\mathfrak{p})}^2 \le C h_c^{-3} \left( \|p\|_{L^2(\mathfrak{p})}^2 + h_c^2 |p|_{H^1(\mathfrak{p})}^2 + h_c^4 |p|_{H^2(\mathfrak{p})}^2 \right). \tag{5.6}$$

The conclusion follows by noticing that $h_c^{-3}\|\mathsf{R}_{\mathcal{P}_c}(p)\|_{2,c}^2 = \sum_{v \in \mathrm{V}_c} |p(\boldsymbol{x}_v)|^2 + |p(\boldsymbol{x}_c)|^2 \le \sum_{\mathfrak{p} \in \mathfrak{P}_c} 2\|p\|_{L^\infty(\mathfrak{p})}^2$.

Let now $c \in \mathrm{C}$, let $p \in H^2(c)$, let $P \in \mathbb{P}_1(c)$, and let us prove Lemma 3.6. We observe that

$$
\begin{aligned}
\|p - \mathcal{I}_{\mathcal{P}_c}(p)\|_{L^2(c)} &\le \|p - P\|_{L^2(c)} + \|\mathcal{I}_{\mathcal{P}_c}(p - P)\|_{L^2(c)} \\
&\le \|p - P\|_{L^2(c)} + C_\sharp \|\mathsf{R}_{\mathcal{P}_c}(p - P)\|_{2,c} \\
&\lesssim \|p - P\|_{L^2(c)} + h_c|p - P|_{H^1(c)} + h_c^2|p - P|_{H^2(c)},
\end{aligned}
$$

using the triangle inequality and Lemma 3.2 on the first line, Lemma 3.1 on the second line, and (5.5) on the third line. Moreover, we observe that

$$
\begin{aligned}
|p - \mathcal{I}_{\mathcal{P}_c}(p)|_{H^1(c)} &\le |p - P|_{H^1(c)} + |\mathcal{I}_{\mathcal{P}_c}(p - P)|_{H^1(c)} \\
&\le |p - P|_{H^1(c)} + C_\mathrm{Inv} h_c^{-1}\|\mathcal{I}_{\mathcal{P}_c}(p - P)\|_{L^2(c)} \\
&\le |p - P|_{H^1(c)} + C_\mathrm{Inv} h_c^{-1}\|p - P\|_{L^2(c)} + C_\mathrm{Inv} h_c^{-1}\|p - \mathcal{I}_{\mathcal{P}_c}(p)\|_{L^2(c)},
\end{aligned}
$$

using the triangle inequality and Lemma 3.2 on the first line, the inverse inequality from Lemma 5.1 on the second line, and again the triangle inequality and Lemma 3.2 on the third line. Combining these two bounds, using that $|p - P|_{H^2(c)} = |p|_{H^2(c)}$ and that $P$ is arbitrary in $\mathbb{P}_1(c)$, we infer that

$$\|p - \mathcal{I}_{\mathcal{P}_c}(p)\|_{L^2(c)} + h_c|p - \mathcal{I}_{\mathcal{P}_c}(p)|_{H^1(c)} \lesssim \inf_{P \in \mathbb{P}_1(c)} (\|p - P\|_{L^2(c)} + h_c|p - P|_{H^1(c)}) + h_c^2|p|_{H^2(c)}.$$

We conclude using the polynomial approximation property from Lemma 5.3. $\qquad\square$

# References

[1] Y. Achdou, C. Bernardi, and F. Coquel. A priori and a posteriori analysis of finite volume discretizations of Darcy's equations. *Numer. Math.*, 96(1):17–42, 2003.

[2] M. Bebendorf. A note on the Poincaré inequality for convex domains. *Z. Anal. Anwendungen*, 22(4):751–756, 2003.

[3] R. Becker and M. Braack. A finite element pressure gradient stabilization for the Stokes equations based on local projections. *CALCOLO*, 38(4):173–199, 2001.

[4] J. Bonelle. *Compatible Discrete Operator schemes on polyhedral meshes for elliptic and Stokes equations.* PhD thesis, Université Paris Est, 2014.

[5] J. Bonelle and A. Ern. Analysis of compatible discrete operator schemes for elliptic problems on polyhedral meshes. *ESAIM Math. Model. Numer. Anal.*, 48(2):553–581, 2014.

[6] M. Braack and E. Burman. Local projection stabilization for the Oseen problem and its interpretation as a variational multiscale method. *SIAM J. Numer. Anal.*, 43(6):2544–2566, 2006.

[7] E. Burman. A unified analysis for conforming and nonconforming stabilized finite element methods using interior penalty. *SIAM J. Numer. Anal.*, 43(5):2012–2033 (electronic), 2005.

[8] E. Burman and A. Ern. Continuous interior penalty *hp*-finite element methods for advection and advection-diffusion equations. *Math. Comp.*, 76(259):1119–1140 (electronic), 2007.

[9] E. Burman and P. Hansbo. Edge stabilization for Galerkin approximations of convection-diffusion-reaction problems. *Comput. Methods Appl. Mech. Engrg.*, 193(15-16):1437–1453, 2004.

[10] E. Burman and F. Schieweck. Local CIP stabilization for composite finite elements. *SIAM J. Numer. Anal.*, 54(3):1967–1992, 2016.

[11] P. Cantin and A. Ern. Vertex-based compatible discrete operator schemes on polyhedral meshes for advection-diffusion equations. *Comput. Meth. Appl. Math.*, 16, 2016.

[12] D. Di Pietro and A. Ern. *Mathematical aspects of discontinuous Galerkin methods*, volume 69 of *Mathématiques & Applications (Berlin) [Mathematics & Applications]*. Springer, Heidelberg, 2012.

[13] A. Ern and J.-L. Guermond. *Theory and practice of finite elements*, volume 159 of *Applied Mathematical Sciences*. Springer-Verlag, New York, 2004.

[14] A. Ern and J.-L. Guermond. Discontinuous Galerkin methods for Friedrichs' systems. II. Second-order elliptic PDEs. *SIAM J. Numer. Anal.*, 44(6):2363–2388, 2006.

[15] A. Ern and J.-L. Guermond. Finite element quasi-interpolation and best approximation. Technical Report http://arxiv.org/abs/1505.06931, arXiv, 2015.

[16] R. Eymard, C. Guichard, and R. Herbin. Small-stencil 3D schemes for diffusive flows in porous media. *ESAIM Math. Model. Numer. Anal.*, 46(2):265–290, 2012.

[17] R. Eymard, C. Guichard, R. Herbin, and R. Masson. Vertex-centred discretization of multiphase compositional Darcy flows on general meshes. *Comput. Geosci.*, 16(4):987–1005, 2012.

[18] R. Eymard, C. Guichard, R. Herbin, and R. Masson. Gradient schemes for two-phase flow in heterogeneous porous media and Richards equation. *ZAMM Z. Angew. Math. Mech.*, 94(7-8):560–585, 2014.

[19] J.-L. Guermond. Stabilization of Galerkin approximations of transport equations by subgrid modeling. *M2AN Math. Model. Numer. Anal.*, 33(6):1293–1316, 1999.

[20] J.-L. Guermond. Subgrid stabilization of Galerkin approximations of linear monotone operators. *IMA J. Numer. Anal.*, 21:165–197, 2001.

[21] C. Johnson, U. Nävert, and J. Pitkäranta. Finite element methods for linear hyperbolic equations. *Comput. Methods Appl. Mech. Engrg.*, 45:285–312, 1984.

[22] C. Johnson and J. Pitkäranta. An analysis of the discontinuous Galerkin method for a scalar hyperbolic equation. *Math. Comp.*, 46(173):1–26, 1986.

[23] P. Lesaint and P.-A. Raviart. On a finite element method for solving the neutron transport equation. In C. de Boors, editor, *Mathematical aspects of Finite Elements in Partial Differential Equations*, pages 89–123. Academic Press, 1974.

[24] G. Matthies, P. Skrzypacz, and L. Tobiska. A unified convergence analysis for local projection stabilisations applied to the Oseen problem. *M2AN Math. Model. Numer. Anal.*, 41(4):713–742, 2007.

[25] G. Matthies, P. Skrzypacz, and L. Tobiska. Stabilization of local projection type applied to convection-diffusion problems with mixed boundary conditions. *Electron. Trans. Numer. Anal.*, 32:90–105, 2008.